Primljen / Received: 16.12.2014.
Ispravljen / Corrected: 13.2.2015.
Prihvaćen / Accepted: 20.2.2015.
Dostupno online / Available online: 10.7.2015.

Effects of seismic zones and site conditions on response of RC buildings

Authors:

Burak Yön, Ph.D. CE
Dicle University, Turkey
Faculty of Engineering
Department of Civil Engineering
burakyon@gmail.com

Assist.Prof. Mehmet Emin Öncü, Ph.D. CE
Dicle University, Turkey
Faculty of Engineering
Department of Civil Engineering
oncume@dicle.edu.tr

Prof. Yusuf Calayır, Ph.D. CE
Fırat University, Turkey
Faculty of Engineering
Department of Civil Engineering
ycalayir@firat.edu.tr

Scientific paper - Subject review

Burak Yön, Mehmet Emin Öncü, Yusuf Calayır

Effects of seismic zones and local soil conditions on response of RC buildings

The effect of seismic zones and local soil conditions given in Turkish Seismic Code on the nonlinear response of reinforced concrete buildings, evaluated using the distributed plastic hinge approach, is investigated in this paper. A RC frame building was selected for numerical analysis, and the nonlinear dynamic time history analyses were performed. For the purposes of analyses, selected earthquake records were adjusted to become compatible with the design response spectrum, taking into account seismic zones and local soil conditions. Interstorey drifts, cross-sectional forces at the base of the building, and energy dissipation for selected hinges, were compared in the paper.

Key words:
seismic zones, local soil conditions, distributed plastic hinges, time history response analysis

Pregledni rad

Burak Yön, Mehmet Emin Öncü, Yusuf Calayır

Utjecaj potresnih zona i lokalnih uvjeta tla na odziv armiranobetonskih zgrada

U radu se preko distribucije plastičnih zglobova istražuje utjecaj potresnih zona i lokalnih uvjeta u tlu, definiranih u turskim potresnim normama na nelinearni odziv armiranobetonskih građevina. Za numeričku analizu je odabrana okvirna armiranobetonska zgrada i izvršeni su nelinearni dinamički proračuni odziva u vremenu. Za potrebe analiza, odabrani zapisi potresa su prilagođeni kako bi odgovarali proračunskom spektru odziva, pri čemu su u obzir uzeta potresna područja i lokalni uvjeti u tlu. U radu su uspoređeni međukatni pomaci, poprečne sile u podnožju zgrade te trošenje energije u odabranim zglobovima.

Ključne riječi:
potresna područja, lokalni uvjeti u tlu, distribuirani plastični zglobovi, proračun odziva u vremenu

Übersichtsarbeit

Burak Yön, Mehmet Emin Öncü, Yusuf Calayır

Einfluss der Erdbebenzonen und lokaler Bodenverhältnisse auf das Verhalten von Stahlbetongebäuden

In dieser Arbeit werden Einflüsse der Erdbebenzonen und lokalen Bodenverhältnisse, die nach türkischen Erdbebennormen definiert sind, auf das nichtlineare Verhalten von Stahlbetongebäuden mittels der Ausbreitung plastischer Gelenke untersucht. Für numerische Analysen ist ein Gebäude mit Stahlbetonrahmen ausgewählt und das nichtlineare dynamische Verhalten im Zeitverlauf ist berechnet. Gegebene Erdbebenaufzeichnungen sind dem Berechnungsspektrum angepasst, wobei Erdbebenzonen und lokale Bodenverhältnisse berücksichtigt sind. Ein Vergleich der Stockwerksverschiebungen, der aufgenommenen Schubkräfte und der Energiedissipation ist für ausgewählte Gelenke aufgestellt.

Schlüsselwörter:
Erdbebenzonen, lokale Bodenverhältnisse, distribuierte plastische Gelenke, Zeitverlaufsanalyse

1. Introduction

Earthquakes rank among the most hazardous natural events that have caused great destruction to human beings and structures ever since the beginning of life. Recent earthquakes such as 1999 Kocaeli earthquake in Turkey, 2003 Bam earthquake in Iran, 2005 Pakistan earthquake in Pakistan, 2008 Wenchuan earthquake in China, 2009 L'Aqulia earthquake in Italy, 2010 Chile earthquake in Chile, 2010 Haiti earthquakes in Haiti, and 2011 Van earthquakes in Turkey, also led to loss of life and property. Many researchers have investigated damage to buildings caused by earthquakes, and they have presented lessons learnt from such natural disasters [1-9]. High seismicity and local site conditions have a considerable effect on building damage [10, 11]. Failures and collapses can increase due to effect of soil with a complex and layered structure. This damage is mainly caused by liquefaction, faulting, and soil amplification. This paper focuses on the effects of seismicity level (from 0.1*g* to 0.4g, where g stands for gravitational acceleration) on nonlinear behaviour of RC buildings. These effects are determined according to seismic zones and local site conditions,defined as Z1, Z2, Z3 and Z4 according to Turkish Seismic Code (TSC) [12]. Therefore, the nonlinear dynamic time history analyses of the selected building were performed. For these analyses, selected earthquake acceleration records were adjusted so as to make them compatible with the design spectra according to the seismicity level and local site conditions. The interstorey drifts, base shear forces of the building, moment-rotation curves, and the amount of energy dissipation at lower ends of two ground floor columns, were obtained according to the adjusted records. The results were compared with each other. The distributed plastic hinge approach was used in nonlinear analysis.

2. Distributed plastic hinge approach

The hinge model accounts for plasticity distributed along to the structural element cross-section, and along its length. In this model, structural elements are divided into three types of fibres: for monitoring nonlinear behaviour of longitudinal steel reinforcing bars, confined concrete consisting of core concrete, and unconfined concrete consisting of cover concrete. Fibre modelling of a typical section of a reinforced concrete element is shown in Figure 1. In nonlinear analysis, structural elements were divided into four members. One hundred section fibres were used for discretization of structural elements. Rayleigh damping was used for damping.

The distributed plastic hinge approach is more accurate than the point hinge models, especially when large axial force variations exist (Mwafy and Elnashai [13]). However, Taucer et al. [14], Petrangeli [15], Jeong and Elnashai [16] validated the accuracy of this model by comparing it with experimental test data. For this reason, the model has been used by researchers. Mwafy [17] evaluated seismic design response factors of concrete wall buildings. For numerical study, five structures were selected and analysed using the distributed hinge modelling. Duan and Hueste [18] evaluated seismic behaviour of a five story reinforced concrete building designed according to Chinese seismic code requirements. They used the distributed hinge model for the analyses. Kwon and Kim [19] assessed a reinforced concrete building damaged during the 2007 Pisco-Chincha earthquake in Peru. They performed the nonlinear analysis of this building using the distributed hinge model. Sarno and Manfredi [20] performed the pushover and dynamic analyses for both constructed and retrofitted buildings to investigate the efficiency of buckling restrained braces. They used the distributed element model in nonlinear analysis. Yön and Calayır [21] performed the pushover analysis of a reinforced concrete building using the lumped and distributed hinge models together with various lateral load patterns. Carvalho et al. [22] investigated comparison of various hinge model approaches by performing the nonlinear static and dynamic analysis of a reinforced-concrete structure. Yön and Calayır [23] investigated effects of the confinement reinforcement and concrete strength on the nonlinear behaviour of reinforced concrete buildings using the distributed hinge model.

The distributed hinge model was used in this study to investigate effects of seismic zones and local site conditions

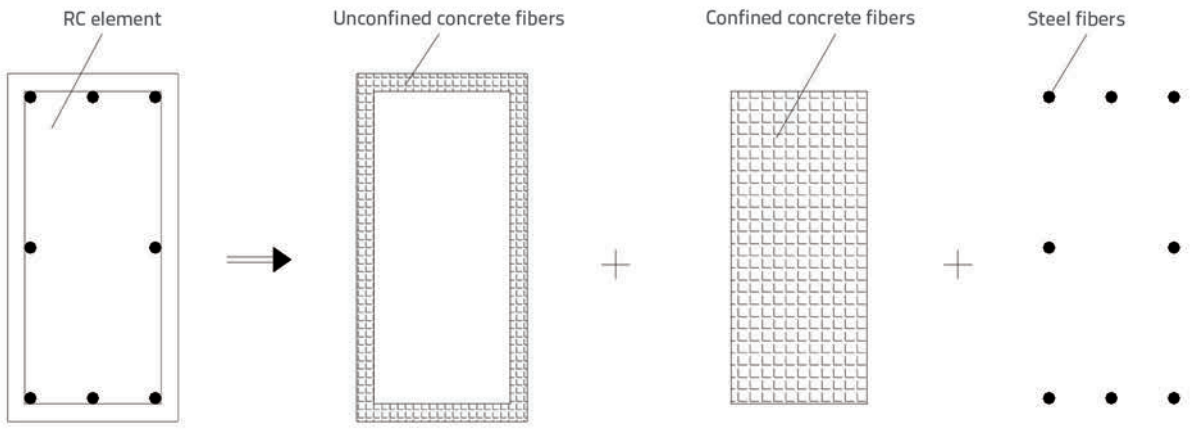

Figure 1. Typical fibre models of a RC element

on reinforced concrete buildings. The SeismoStruct program [24], which can simulate the inelastic response of structural systems subjected to static and dynamic loads, was used for nonlinear analyses. Also, the SeismoArtif [25] program was used to scale earthquake acceleration records to design spectrums.

3. Numerical analysis

3.1. Building description and material properties

A 5-storey and 4-bay reinforced concrete frame with high ductility was selected for numerical application. The total height of the building is 18.5 meters. The height of the first story of the building is 4.5 m, and the height of each of the other storeys is 3.5 m. The column dimensions were selected as 50x50 cm, and dimensions for beams were selected as 25x50 and 30x60 cm, in the middle bay and in other bays, respectively. The slab thickness of 12 cm was selected. The building was analysed according to seismic zones and local site conditions indicated in TSC. It was assumed that the building importance coefficient is 1.0, and that the concrete class is C25, while the reinforcing steel class is S420. The elevation of the selected frame building and the cross sections of structural elements are given in Figure 2. Four Gauss integration points were selected to calculate the element forces and the stress–strain relationship for each section. In this building, the superimposed dead load and the live load required by the Turkish Standard 498 [26] were adopted as 1.5 kPa and 2.0 kPa, respectively. The base of the building was assumed to be rigidly fixed, and the soil compliance and damping properties were not taken into account.

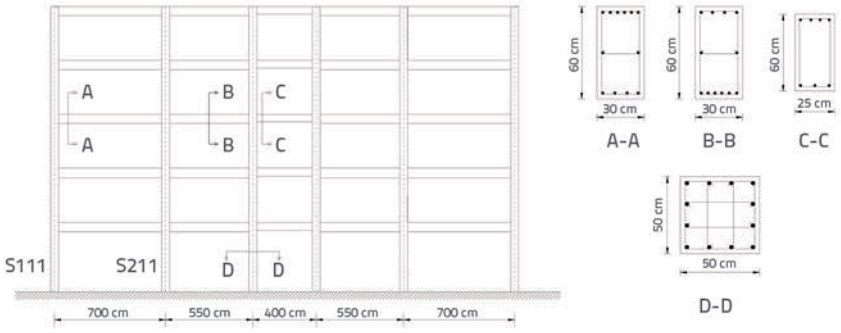

Figure 2. Elevation of the building, column and beam cross sections

Table 1. Parameters related to confinement zones in structural elements

Structural elements		Longitudinal reinforcement	Transverse reinforcement spacing [cm]	Length of confinement zone [cm]	Confinement factor
Column	Confinement zone of column	12Ø16	10	80	1.2970
	Central zone of column		15		1.1817
Beam	Confinement zone of beam	Top reinforcement 6Ø14	10	120	1.1400
	Central zone of beam	Bottom reinforcement 4Ø14	20		1.0452
Beam	Confinement zone of beam	Top reinforcement 5Ø14	10	100	1.0085
	Central zone of beam	Bottom reinforcement 4Ø14	20		1.0021

Table 2. Performance criteria used in analyses

Damage level	Limit values for confined concrete	Limit values for unconfined concrete	Limit values for steel bar
Minimum damage limit (MN)	$(\varepsilon_{cu})_{MN} = 0{,}0035$	0.0035	$(\varepsilon_s)_{MN} = 0{,}010$
Safety damage limit (GV)	$(\varepsilon_{cg})_{GV} = 0{,}0035 + 0{,}01\left(\frac{\rho_s}{\rho_{sm}}\right) \le 0{,}0135$	0.0037	$(\varepsilon_s)_{GV} = 0{,}040$
Collapse damage limit (GC)	$(\varepsilon_{cg})_{GC} = 0{,}004 + 0{,}014\left(\frac{\rho_s}{\rho_{sm}}\right) \le 0{,}018$	0.0040	$(\varepsilon_s)_{GC} = 0{,}060$

The bilinear elastic plastic material model, which includes kinematic strain hardening, was used for reinforcing bars. Concrete material was defined by the uniaxial confinement concrete model. The confinement effect was calculated using the Mander model (Mander et al. [27]). Parameters relating to confinement zones in structural elements are presented in Table 1.

3.2. Failure Criteria

Seismic performance criteria are based on TSC. Three damage limit levels [Minimum Damage Limit (MN), Safety Damage Limit (GV) and Collapse Damage Limit (GC)], as defined in TSC, were used for seismic evaluation. These limit values are shown in Table 2.

In Table 2, the value ε_{cu} represents the ultimate strain of unconfined concrete, while ε_{cg} illustrates the ultimate strain of confined concrete. Also, ε_s represents deformation of the reinforcement steel unit. The ρ_s is the volumetric ratio of spiral reinforcement present in the cross section and arranged as "special seismic hoops and crossties", while ρ_{sm} defines volumetric ratio of the transverse reinforcement that must be present in the cross section [12].

3.3. Earthquake parameters and local site conditions

Selected earthquake accelerations properties are given in Table 3. The seismic records were obtained from the PEER Strong Motion Database [28] and these records were scaled in frequency content in order to be compatible with the target design spectrum according to seismic zones and local site conditions in TSC.
Spectrum characteristic periods according to the soil classes (from Z1 to Z4) and soil groups are presented in Tables 4 and 5, respectively. In addition, the elastic response spectrums, plotted according to local site classes, are given in Figure 3.

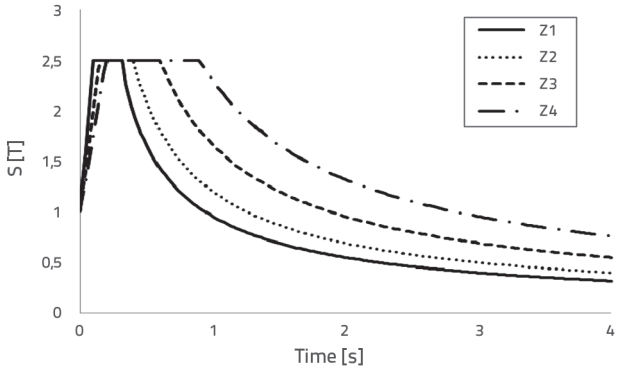

Figure 3. Recommended elastic response spectra for ground types Z1 to Z4 in TSC (for 5 % damping)

Table 3. Selected earthquake acceleration records for dynamic analysis

Earthquakes	Station	Direction	Date	Magnitude	PGA [g]	Duration [s]
Kocaeli	Düzce	N-S	August 17, 1999	7,4	0,358	26,44
Loma Prieta	Corralitos	E-W	October 18, 1989	6,9	0,644	40,0
Imperial Valley	El Centro Array	E-W	May 19, 1940	7,0	0,313	40,0
PGA - Peak ground acceleration						

Table 4. Spectrum characteristic periods according to the soil classes in TSC

Local site classes	T_A [s]	T_B [s]	Soil groups and topmost soil layer thickness
Z1	0,10	0,30	Group (A) soils ; Group (B) soils with $h_1 \leq 15$ m
Z2	0,15	0,40	Group (B) soils with $h_1 > 15$ m ; Group (C) soils with $h_1 \leq 15$ m
Z3	0,15	0,60	Group (C) soils with $15 \text{ m} < h_1 \leq 50$ m ; Group (D) soils with $h_1 \leq 10$ m
Z4	0,20	0,90	Group (C) soils with $h_1 > 50$ m ; Group (D) soils with $h_1 > 10$ m

Table 5. Soil Groups defined in TSC, [12]

Soil groups	Description of soil group	Standard penetration (N/30)	Relative density [%]	Unconfined compressive strength [kPa]	Shear wave velocity [m/s]
A	1. Massive volcanic rocks, unweathered sound metamorphic rocks, stiff cemented sedimentary rocks	-	-	> 1000	> 1000
	2. Very dense sand, gravel...	> 50	85-100	-	> 700
	3. Hard clay and silty clay...	> 32	-	> 400	> 700
B	1. Soft volcanic rocks such as tuff and agglomerate, weathered cemented sedimentary rocks with planes of discontinuity.....	-	-	500-1000	700-1000
	2. Dense sand, gravel.....	30-50	65-85	-	400-700
	3. Very stiff clay, silty clay...	16-32	-	200-400	300- 700
C	1. Highly weathered soft metamorphic rocks and cemented sedimentary rocks with planes of discontinuity	-	-	< 500	400-700
	2. Medium dense sand and gravel....	10-30	35-65	-	200-400
	3. Stiff clay and silty clay.....	8-16	-	100-200	200-300
D	1. Soft, deep alluvial layers with high ground water level	-	-	-	< 200
	2. Loose sand.....	< 10	< 35	-	< 200
	3. Soft clay and silty clay.....	< 8	-	< 100	< 200

When comparing the TSC response spectra with those contained in Eurocode (EC-8) [29], we can see that there are four soil classes in TSC (Z1, Z2, Z3 and Z4), while there are seven soil types in EC-8 (A, B, C, D, E, S1 and S2). Soil typesS1 and S2 identified in EC-8 are described as special soil types. Special investigations have to be carried out for determination of seismic load in regions that have soil types S1 and S2. Soil failure under seismic load should especially be considered for the soil type S2. Also, EC-8 proposes two spectra: Type 1 and Type 2. Type 2 spectrum should be used if ground wave magnitudes Ms, which involve most of seismic hazards identified in a region, are smaller than 5.5. These spectra are shown in Figure 4a-b. In these figures, S_e, a_g and $T(S)$ show the elastic response spectrum, design ground acceleration, and vibration period of a linear single degree of freedom system, respectively.

According to the Seismic Zone Map prepared in 1996 by the Ministry of Public Works and Settlement, Turkey is divided into 5 seismic zones. According to TSC, the first degree earthquake zone is the most hazardous and the fifth zone is the zone with no hazard. The code requires ground acceleration from 0.1g to 0.4g for buildings located in the first and the fourth degree earthquake zones, respectively. This map is shown in Figure 5. Predominant periods obtained from SeismoSignal [30] of the original records, the building and the scaled records for 0.3*g* and 0.4*g* ground accelerations are shown in Table 6. In addition, design spectra obtained by multiplying the elastic spectrum with ground accelerations and building important factor, taking into account the local site conditions, are given in Figure 6a-d. Thus, the effect of seismic zone degrees and local site conditions of the building response are taken into account.

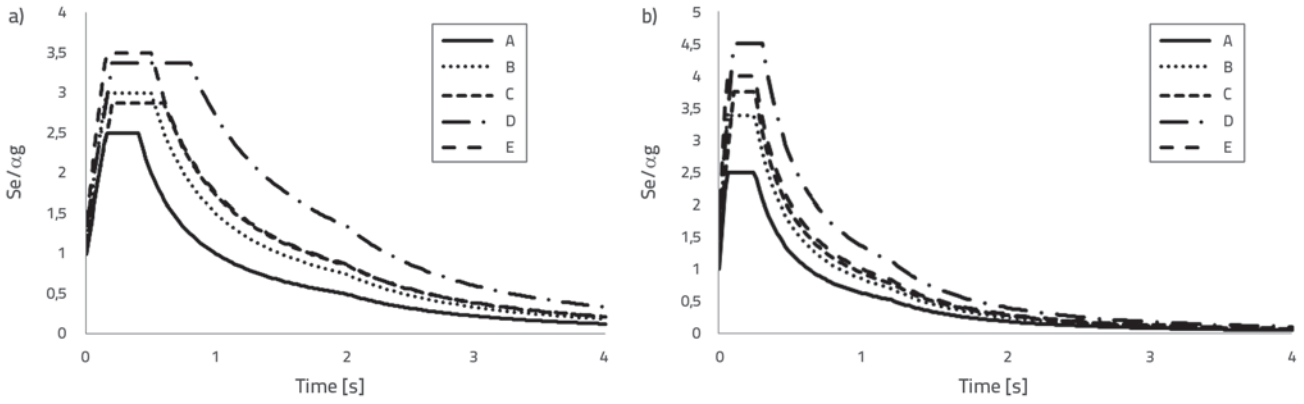

Figure 4. Recommended Type elastic response spectra for ground types A to E in EC-8 (5 % damping): a) Type 1; b) Type 2

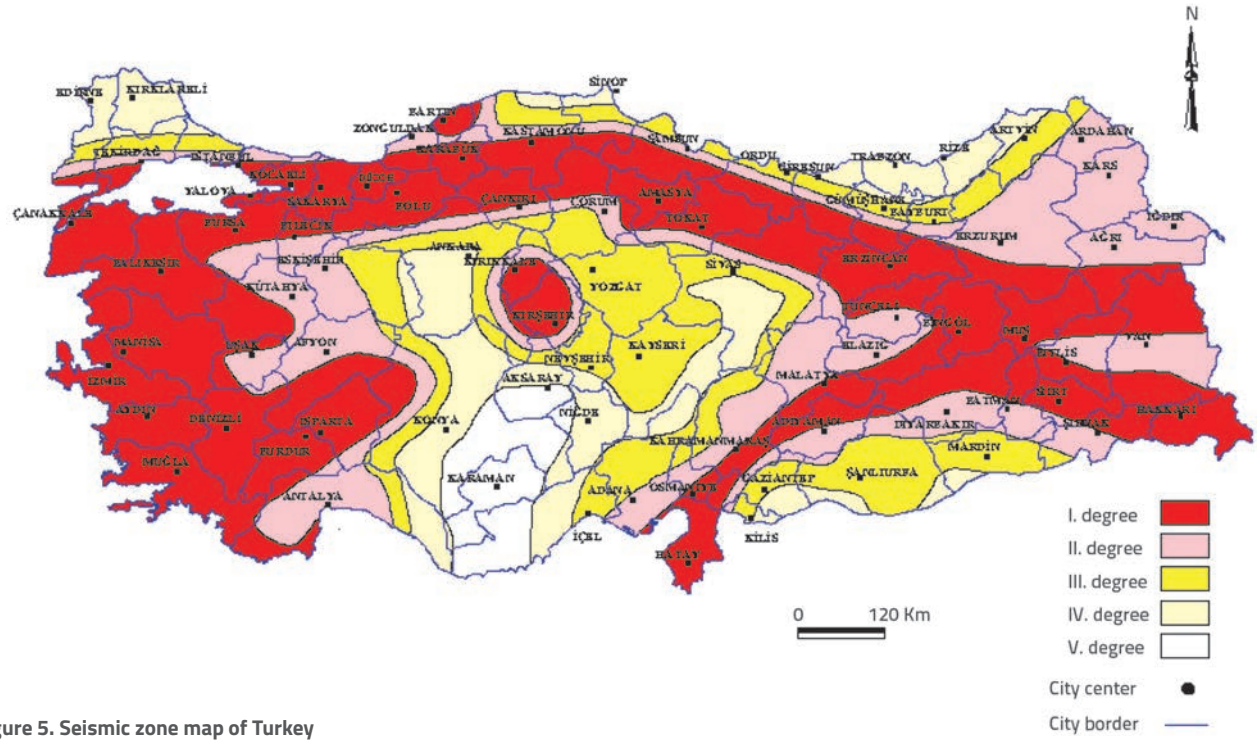

Figure 5. Seismic zone map of Turkey

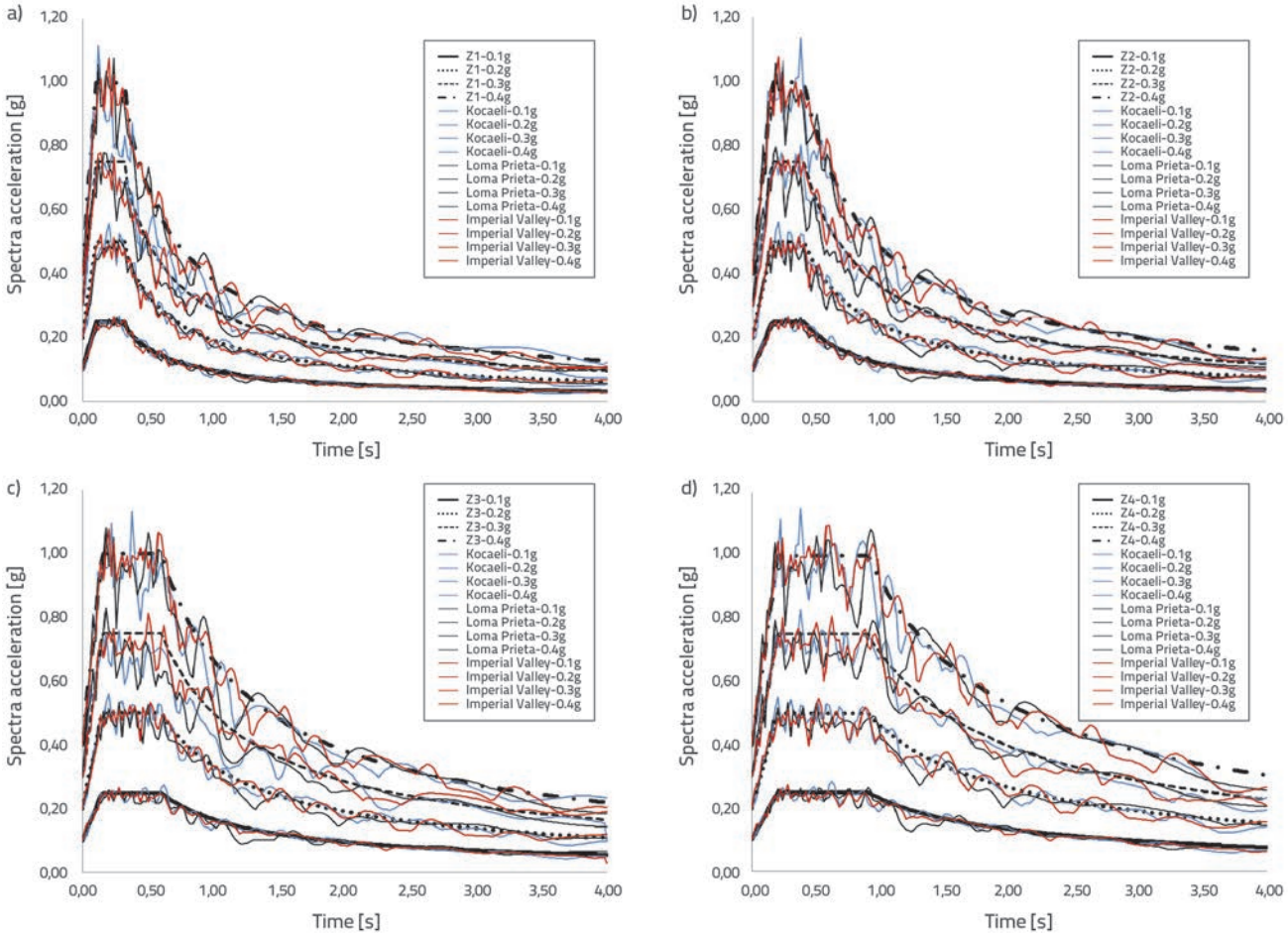

Figure 6. Response spectra of the earthquake acceleration records scaled according to the elastic design spectrum for four soil classes with ground accelerations defined in TSC

Table 6. Predominant periods of original and scaled records and building

Earthquakes	Predominant periods [s]								
	Original records	Scaled records according to soil classes and ground accelerations							Building
		Z1		Z2		Z3		Z4	
		0,3 g	0,4 g	0,3 g	0,4 g	0,3 g	0,4 g	0,3 g	0,4 g	
Kocaeli	0,28	0,20	0,28	0,28	0,28	0,40	0,60	0,90	0,86	0,9191
Loma Prieta	0,30	0,24	0,24	0,30	0,36	0,40	0,44	0,96	0,92	
Imperial Valley	0,46	0,26	0,24	0,36	0,30	0,50	0,52	0,86	0,82	

It can be seen from Table 6 that the increase of soil class from Z1 to Z4 significantly enhances the predominant period of earthquakes. Thus, predominant periods of the scaled records for Z3 and Z4 soil classes are close to first natural period of the building.

4. Results of numerical analysis

Base shear forces of the building, for various local site conditions and ground accelerations, are presented in Figure 7-9. It can be seen from these figures that the base shear forces have an increasing tendency from Z1 to Z4 for the same ground acceleration. However, these increase ratios differ according to earthquake characteristics. As shown in these figures, greatest differences for base shear forces according to different local site conditions for the same ground acceleration were obtained from the scaled Imperial Valley records. It can be seen that local site conditions are more effective than ground acceleration in terms of base shear forces.

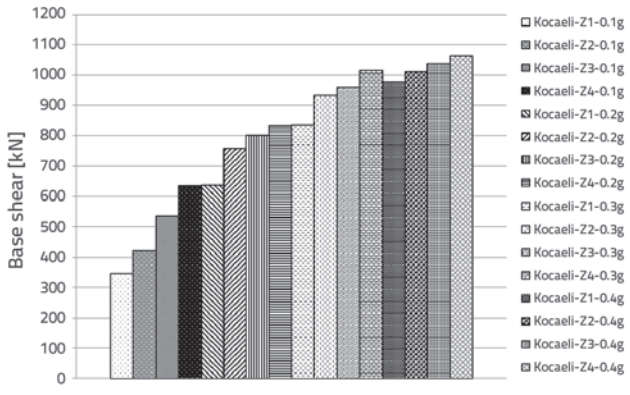

Figure 7. Base shear forces of Kocaeli earthquake acceleration records scaled according to the elastic design spectrum for four soil classes with ground accelerations defined in TSC

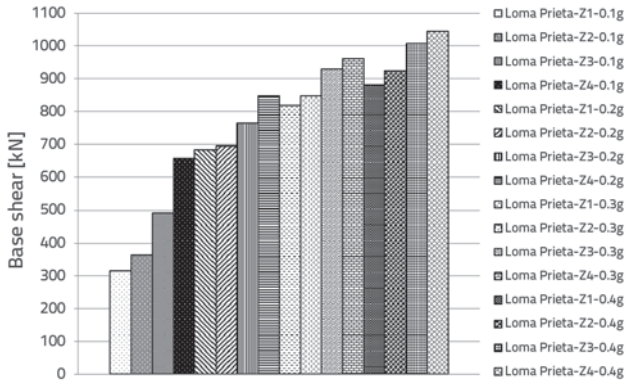

Figure 8. Base shear forces of Loma Prieta earthquake acceleration records scaled according to the elastic design spectrum for four soil classes with ground accelerations defined in TSC

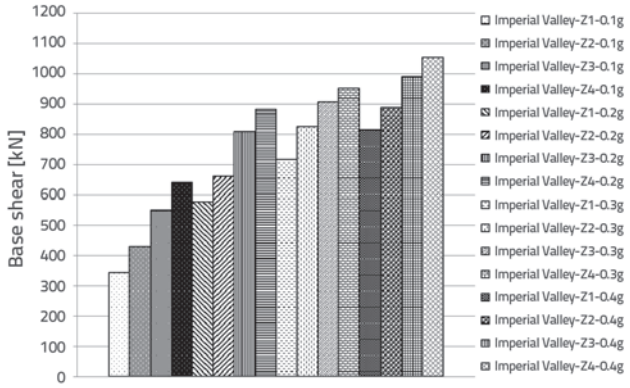

Figure 9. Base shear forces of Imperial Valley earthquake acceleration records scaled according to the elastic design spectrum for four soil classes with ground accelerations defined in TSC

The effective interstorey drift ratio, amounting to 2 % according to TSC, and interstorey drifts of the building for various local site conditions, with ground accelerations, are presented in Figure 10-12.

Interstorey drifts obtained using the scaled Kocaeli earthquake are shown in Figure 10. For this scaled earthquake, the largest interstorey drift ratios were obtained for Z4 soil class with 0.4*g*, for Z3 soil class with 0.4g, for Z4 soil class with 0.3g, and for Z3 soil class with 0.3*g* ground accelerations. In these cases, the interstorey drift ratios ranged from 3.0 % to 4.25 %. However, the smallest interstorey drifts were obtained for Z1 soil class with 0.1*g*, for Z2 soil class with 0.1*g*, for Z3 soil class with 0.1*g*, and for Z1 soil class with 0.2*g*. In these cases, the interstorey drift ratios ranged from 0.25 % to 0.75 %. These results show that the largest interstorey drift ratio with the 0.4*g* ground acceleration for Z4 soil class is 17 times larger than the smallest interstorey drift with 0.1g ground acceleration for Z1 soil class. Also, the ground floor drifts for Z3 and Z4 soil classes with 0.4g ground acceleration are approximately 2 times larger than interstorey drifts for Z1 and Z2 soil classes with 0.4*g* ground acceleration.

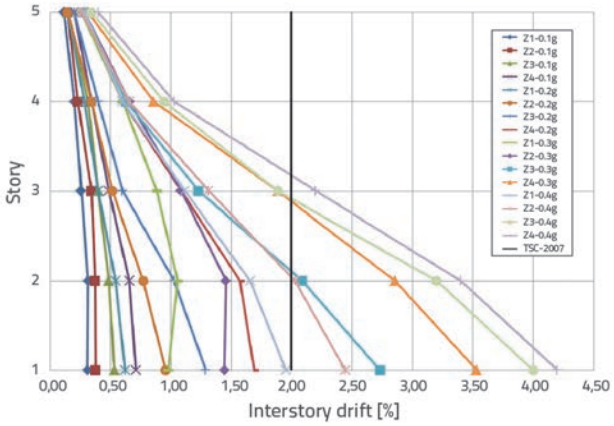

Figure 10. Interstorey drifts of Kocaeli earthquake acceleration records scaled according to the elastic design spectrum for four soil classes with ground accelerations

Interstorey drifts obtained using the scaled Loma Prieta earthquake are given in Figure 11. For this scaled earthquake, the largest interstorey drift ratios at the ground floor were obtained for Z4 soil class with 0.4*g*, for Z3 soil class with 0.4*g*, for Z4 soil class with 0.3*g* and for Z3 soil class with 0.3*g* ground accelerations. The interstorey drift ratios varied between 2.75 % and 5.0 %. However, the smallest interstorey drifts were obtained for Z1 soil class with 0.1*g*, for Z2 soil class with 0.1*g*, for Z3 soil class with 0.1*g*, and for Z1 soil class with 0.2*g*. The interstorey drift ratios varied between 0.25 % and 0.75 %. These results show that the largest interstorey drift ratio registered for Z4 soil class with 0.4*g* ground acceleration is 20 times larger than the smallest interstorey drift registered for Z1 soil class with 0.1g ground acceleration. Also, ground floor drifts for Z3 and Z4 soil classes with 0.4*g* ground acceleration are approximately 2 to 2.25 times larger than the drifts for soil classes Z1 and Z2 with 0.4*g* ground acceleration.

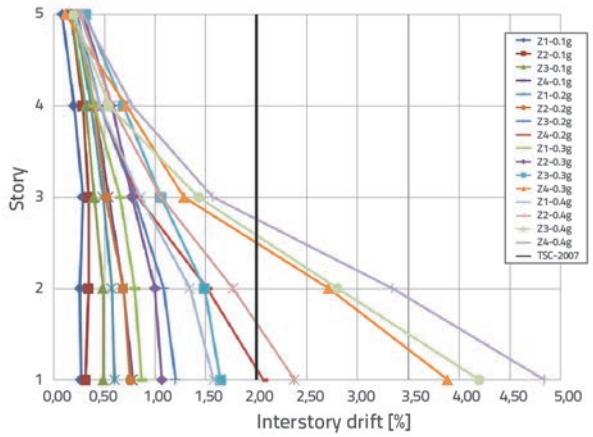

Figure 11. Interstorey drifts of Loma Prieta earthquake acceleration records scaled according to the elastic design spectrum for four soil classes with ground acceleration

Figure 12 shows interstorey drifts obtained from the scaled Imperial Valley earthquake. According to the earthquake, the largest interstorey drift ratios at the ground floor were obtained for Z4 soil class with 0.4g, for Z3 soil class with 0.4*g*, for Z4 soil class with 0.3*g*, and for Z3 soil class with 0.3*g* ground accelerations. The interstorey drifts ratios amounting to 2.8 % and 5.0 % were obtained for these cases. In addition, smaller interstorey drifts were generally obtained for the 0.1*g* ground acceleration for various soil classes. Interstorey drift ratios varied between 0.25 % and 0.75 % for these cases. These results show that the largest interstorey drift ratio, registered for Z4 soil class at 0.4*g* ground acceleration, is 20 times larger than the smallest interstorey drift registered for Z1 soil class with the 0.1g ground acceleration. Also, ground floor interstorey drifts for Z3 and Z4 soil classes with 0.4*g* ground acceleration are approximately 1.8 times larger compared to interstorey drifts for Z1 and Z2 soil classes with 0.4*g* ground acceleration. The obtained interstorey drifts were compared to the interstorey limit defined in TSC and it was established that the drifts in Z3 and Z4 soil classes for 0.3*g* and 0.4g ground accelerations exceed the limit value.

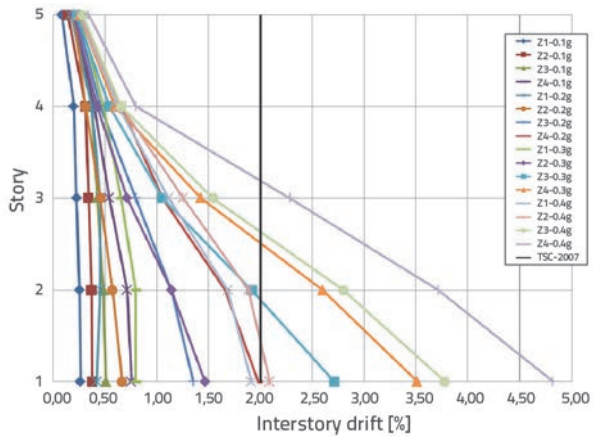

Figure 12. Interstorey drifts of Imperial Valley earthquake acceleration records scaled according to the elastic design spectrum for four soil classes with ground acceleration

Moment-rotation curves were obtained according to various local soil conditions and the maximum ground acceleration (0.4*g*) for lower end of the ground-floor S111 column. These curves are given in Figures 13-15. Moment-rotation curves obtained using the scaled Kocaeli earthquake are shown in Figure 13. It can be seen that absolute maximum moment values occur at the level of 500 kNm, while absolute maximum rotations occur at the level of 0.025 rad at Z3 and Z4 soil classes for the 0.4*g* ground acceleration. However, at the Z2 soil class the maximum moment occurs at the level of 500 kNm and the maximum rotation occurs at the level of 0.15 rad. For the Z1 soil class, the moment is similar to that of other soil classes, and the rotation occurs at the level of 0.10 rad.

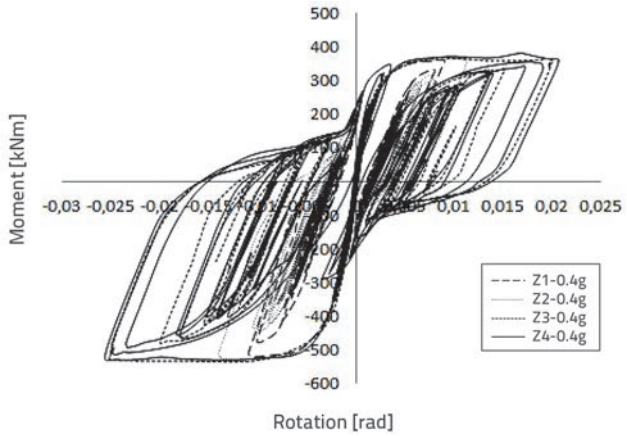

Figure 13. Moment-rotation curves at the lower end of the S111 ground floor column according to scaled Kocaeli earthquake acceleration records for four soil classes with 0.4g ground acceleration

Moment-rotation curves obtained using the scaled Loma Prieta earthquake are given in Figure 14. According to the results, absolute maximum moments for 0.4*g* are equal for all soil types, and this value amounts to approximately 500 kNm. In terms of rotation, the absolute maximum rotation for the Z4 soil class occurs at the level of 0.030 rad, while for Z3 the rotation occurs at the level of 0.025 rad. However, for the Z2 soil class the maximum rotation occurs at the level of 0.015 rad, while for the Z1 soil class the rotation occurs at the level of 0.010 rad.

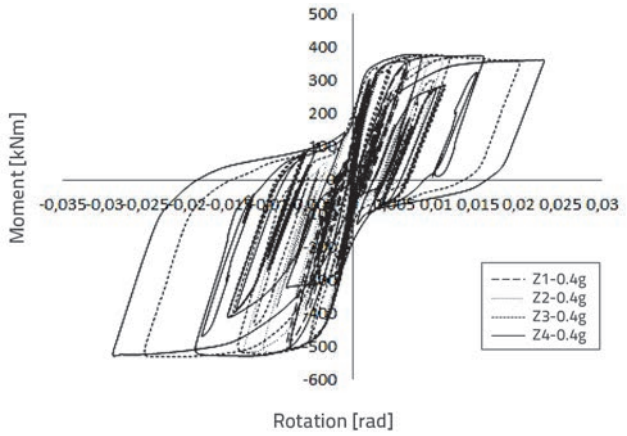

Figure 14. Moment-rotation curves at the lower end of the S111 ground floor column according to the scaled Loma Prieta earthquake acceleration records for four soil classes with the 0.4g ground acceleration

Moment-rotation curves obtained from the scaled Imperial Valley earthquake are given in Figure 15. The results obtained show that absolute maximum moments are equal to 500 kNm for the maximum ground acceleration and for all soil classes. Absolute maximum rotations occur at the level of 0.030, 0.020, 0.010, and 0.005 rad for Z4, Z3, Z2, and Z1 soil classes, respectively.

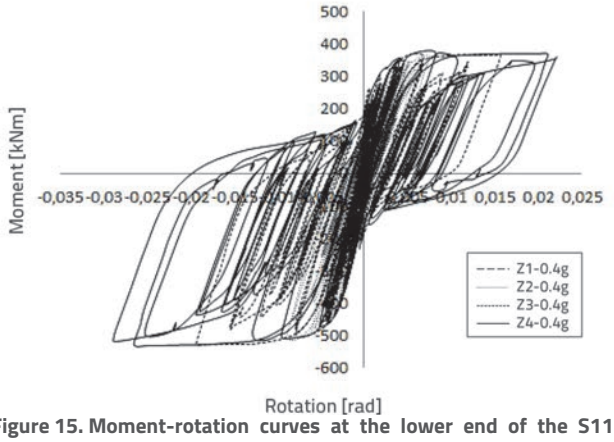

Figure 15. Moment-rotation curves at the lower end of the S111 ground floor column according to the scaled Imperial Valley earthquake acceleration records for four soil classes with the 0.4g ground acceleration

Moment-rotation curves were obtained according to various ground accelerations and the soft soil class (Z4) for the lower end of the ground-floor S211 column. The moment-rotation curves are given in Figures 16-18. Moment-rotation curves obtained using the scaled Kocaeli earthquake are shown in Figure 16 for the Z4 soil class and various ground accelerations. It can be seen that absolute maximum moment values occur at the level of 550 kNm, while absolute maximum rotations occur at the level of 0.025 rad for the 0.4*g* ground acceleration. However, for the 0.3*g* acceleration, the maximum moment occurs at the level of 550 kNm and maximum rotation occurs at the level of 0.15 rad. Similar moments were obtained for the 0.1*g* and 0.2*g* accelerations. In addition, 0.005 rad rotations were registered at these accelerations.

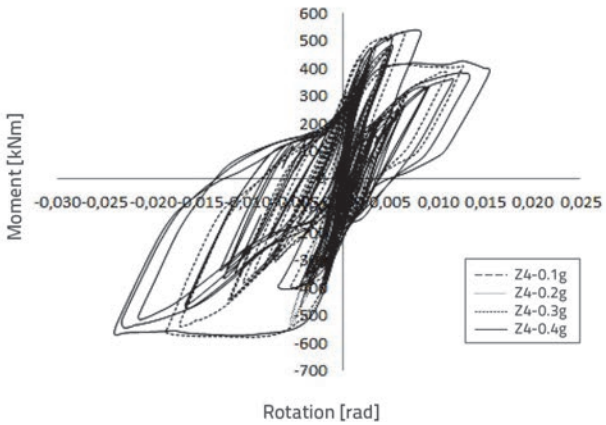

Figure 16. Moment-rotation curves for the lower end of the S211 ground floor column according to the scaled Kocaeli earthquake acceleration records for four ground accelerations in Z4 soil class

Moment-rotation curves determined according to the Z4 soil class and various ground accelerations using the scaled Loma Prieta earthquake are shown in Figure 17. According to the results, absolute maximum moments for all ground accelerations and for the Z4 soil class occurred at approximately 550 kNm. However, the absolute maximum rotation occurs at the level of 0.030 rad for the 0.4*g* ground acceleration. For the 0.3g acceleration, the absolute maximum rotation value is 0.015 rad. Also, the 0.010 rad and 0.005 rad rotations were registered for the 0.2*g* and 0.1*g* ground accelerations, respectively.

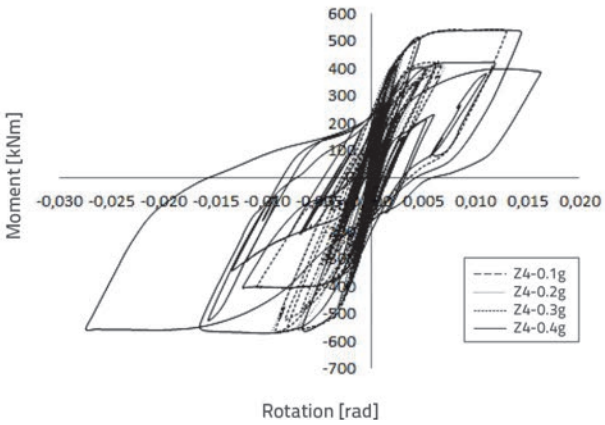

Figure 17. Moment-rotation curves at the lower end of the S211 ground floor column according to the scaled Loma Prieta earthquake acceleration records for four ground accelerations in soil class Z4

Moment-rotation curves for the lower end of the S211 ground floor column, obtained using the scaled Imperial Valley earthquake, are shown in Figure 18. According to the results, absolute maximum moments are very distinct and occur at the level of 550 kNm for the Z4 soil class and for all ground accelerations. Absolute maximum rotations occur at the level of 0.025, 0.020, and 0.005 rad for 0.4*g*, 0.3*g*, 0.2*g*, and 0.1*g* ground accelerations, respectively.

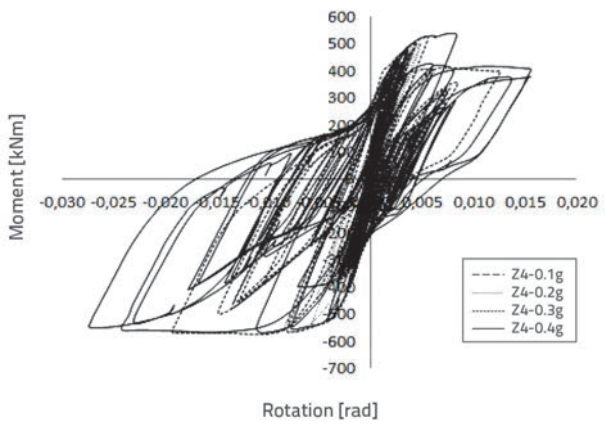

Figure 18. Moment-rotation curves at the lower end of the S211 ground floor column according to the scaled Imperial Valley earthquake acceleration records for four ground accelerations in Z4 soil class

Table 7a. Energy dissipation rate for the 0.4g ground acceleration and various soil classes

Selected hinge	Earthquakes	Amount of energy [kNm]			
		Ground acceleration = 0.4 g			
			Z2	Z3	Z4
Lower end of S111	Kocaeli	8.312	13.597	32.392	57.777
	Loma Prieta	4.826	10.816	26.931	40.868
	Imperial Valley	3.869	8.696	27.230	61.294

Table 7b. Energy dissipation rate for the Z4 soil class and various ground accelerations

Selected hinge	Earthquakes	Amount of energy [kNm]			
		Z4 soil class			
		0.1*g*	0.2*g*	0.3*g*	0.4*g*
Lower end of S211	Kocaeli	2.919	7.410	32.612	59.414
	Loma Prieta	2.601	9.194	20.391	44.293
	Imperial Valley	2.207	12.472	38.542	63.665

The amount of energy dissipated in hinges at the lower end of the ground floor columns S111 and S211, for the 0.4*g* ground acceleration at various soil classes and for the Z4 soil class with various ground accelerations are shown in Tables 7a and 7b. It can be seen from the table that, for the lower end of the S111 ground column and for the 0.4*g* scaled earthquakes, the amount of energy dissipation increases approximately from 7 to 20 times for the ratio of Z4/Z1 soil classes. However, for the lower end of the S211 ground column, and for the Z4 soil class, the amount of energy dissipation increases from 20 to 30 times for the ratio of 0.4*g*/0.1*g* ground accelerations of the scaled earthquakes.

In TSC, the damage is determined according to deformation levels. The limitations are presented in Table 2 according to damage levels for cover concrete, core concrete, and steel bar. Figures 19 and 20 show damage limits for confined concrete and steel bar, and deformations according to the scaled earthquake records at lower ends of the S111 and S211 ground floor columns. It can be seen from these figures that, for the lower end of the S111 column, the deformations obtained from the 0.4*g* ground acceleration for Z3 and Z4 soil classes exceed the collapse damage limit (GC) for confined concrete. However, minimum deformations occur in the Z1 soil class with the 0.4*g* ground acceleration, and these values remain below the limit of minimum damage (MN) for steel bars. For the lower end of the S211 column, deformations obtained from Z4 soil class for 0.4 ground acceleration exceed the collapse

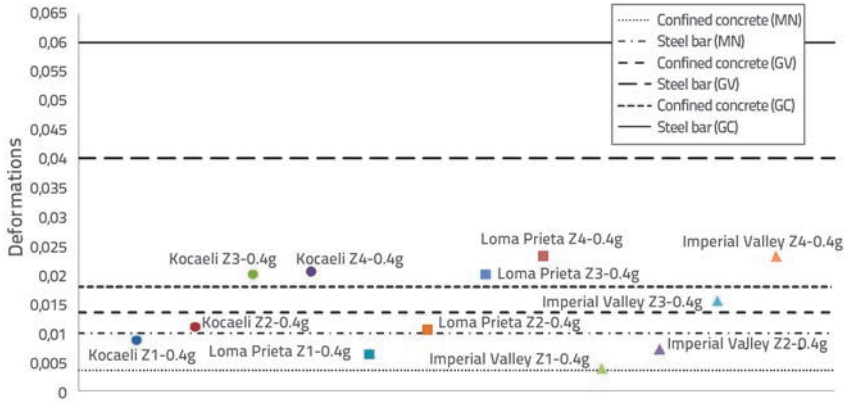

Figure 19. Damage limits and occurred deformations according to scaled earthquakes for lower end of S111 ground column

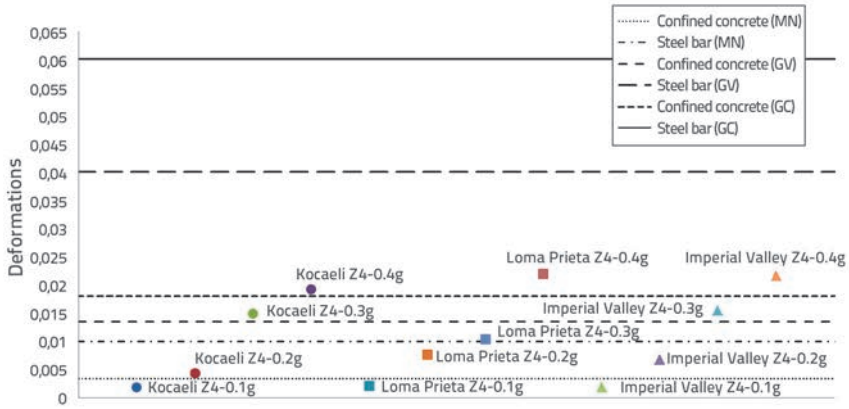

Figure 20. Damage limits and deformations registered according to scaled earthquakes for the lower end of the S211 ground column

damage limit (GC) for confined concrete. Minimum deformations occur in Z4 soil class with 0.1g ground acceleration, and these values remain below the limit of minimum damage (MN) for confined concrete.

4. Conclusions

The effect of seismic zones and local site conditions, as defined in Turkish Seismic Code (TSC), on the nonlinear seismic behaviour of reinforced concrete buildings, was investigated in this paper using the distributed plastic hinge model. For numerical study, a sample reinforced concrete frame building was selected, and nonlinear dynamic time history analyses were performed. Three earthquake acceleration records were selected and adjusted to be compatible with the design spectrum defined in TSC by considering seismic zones and local site conditions for nonlinear analyses. Interstorey drifts, base shear forces of the building, moment-rotation curves, and energy dissipation at lower ends of two ground floor columns, were compared. The following conclusions can be made from the results:

- The increase in soil class from Z1 to Z4 significantly enhances the predominant period of earthquakes. Thus, predominant periods of scaled records for soil classes Z3 and Z4 are close to the first natural period of the building. Consequently, earthquakes are highly destructive to buildings.
- Base shear forces tend to increase from Z1 to Z4 for same ground accelerations. Also, it was determined that the increasing ratios of base shear forces vary according to earthquake characteristics.
- In terms of interstorey drift ratios, the seismicity levels are critical for soft soil classes. However, soil classes can be relatively more critical than the seismicity levels in case of a lower amplitude earthquake for the investigated building.
- Absolute maximum moment values are almost equal for all soil classes under maximum ground acceleration, while absolute maximum rotation values vary in nonlinear analyses of the building according to selected earthquakes.
- Absolute maximum moment values are almost equal under various ground accelerations in case of the same soil class because they reach their capacity moments, while absolute maximum rotation values vary for the building.
- The amount of energy dissipation increases significantly depending on the increase of soil classes and ground accelerations.
- Maximum deformations were obtained for 0.3*g* and 0.4*g*ground accelerations for the soil class Z4 and this for all selected records. However, minimum deformations occurred in soil classes Z4 and Z1 for 0.1g and 0.4g ground accelerations, respectively.

The results show that the nonlinear response of reinforced concrete buildings is considerably affected by seismic zones and local soil conditions. Consequently, seismic zones should be considered together with local soil conditions when designing new reinforced concrete buildings or evaluating existing buildings.

Acknowledgments

The authors gratefully extend their thanks and appreciation to Seismosoft for providing free academic license for SeismoStruct and SeismoArtif software and trial version of SeismiSignal.

REFERENCES

[1] Sezen, H., Whittaker, A.S., Elwood, K.J., Mosalam, K.M.: Performance of reinforced concrete buildings during the August 17, 1999 Kocaeli, Turkey earthquake, and seismic design and construction practice in Turkey, Engineering Structures, 25(1), pp.103-114, 2003., http://dx.doi.org/10.1016/S0141-0296(02)00121-9

[2] Doğangün, A.: Performance of reinforced concrete buildings during the May 1, 2003 Bingöl earthquake in Turkey, Engineering Structures, 26(6), pp. 841-856, 2004., http://dx.doi.org/10.1016/j.engstruct.2004.02.005

[3] Kim, S.J., Elnashai, A.S.: Characterization of shaking intensity distribution and seismic assessment of RC buildings for the Kashmir (Pakistan) earthquake of October 2005, Engineering Structures, 31, pp. 2998-3015, 2009., http://dx.doi.org/10.1016/j.engstruct.2009.08.001

[4] Zhao, B., Taucer, F., Rossetto, T.: Field investigation on the performance of building structures during the 12 May 2008 Wenchuan earthquake in China, Engineering Structures, 31, pp. 1707-1723, 2009., http://dx.doi.org/10.1016/j.engstruct.2009.02.039

[5] Rojas, F., Naeim, F., Lew, M., Carpenter, L.D., Youssef, N.F., Saragoni, G. R., Adaros, M.S.: Performance of tall buildings in Concepción during the 27 February 2010 moment magnitude 8.8 offshore Maule, Chile earthquake, The Structural Design of Tall and Special Buildings, 20, pp. 37-64, 2011., http://dx.doi.org/10.1002/tal.674

[6] O'Brien, P., Eberhard, M., Haraldsson, O,.Irfanoglu, A., Lattanzi, D., Lauer, S., Pujol, S.: Measures of the Seismic Vulnerability of Reinforced Concrete Buildings in Haiti, Earthquake Spectra, 27 (SI), pp. 373-386, 2011.

[7] Calayır, Y., Sayın, E., Yön, B.: Performance of structures in the rural area during the March 8, 2010 Elazığ-Kovancılar earthquake, Natural Hazards, 61(2), pp. 703-717, 2012., http://dx.doi.org/10.1007/s11069-011-0056-6

[8] Bayraktar, A., Altunışık, A.C., Pehlivan, M.: Performance and damages of reinforced concrete buildings during the October 23 and November 9, 2011 Van, Turkey, earthquakes, Soil Dynamics and Earthquake Engineering 53, pp. 49-72, 2013., http://dx.doi.org/10.1016/j.soildyn.2013.06.004

[9] Yön, B., Sayın, E., Köksal, T.S.: Seismic response of buildings during the May 19, 2011 Simav, Turkey earthquake, Earthquakes and Structures, 5 (3), pp. 343-357, 2013., http://dx.doi.org/10.12989/eas.2013.5.3.343

[10] Galal, K., Naimi, M.: Effect of soil conditions on the response of reinforced concrete tall structures to near fault earthquakes, The Structural Design of Tall and Special Buildings, 17, pp. 541–562, 2008., http://dx.doi.org/10.1002/tal.365

[11] Jiang, H., Lu, X., Chen, L.: Seismic fragility assessment of RC moment-resisting frames designed according to current Chinese seismic design code, Journal of Asian Architecture and Building Engineering, 11-1, pp. 153-160, 2012.

[12] Turkish Seismic Code, Ankara, Turkey, 2007.

[13] Mwafy, A.M., Elnashai, A.S.: Static pushover versus dynamic collapse analysis of RC buildings, Engineering Structures, 23, pp. 407–424, 2001., http://dx.doi.org/10.1016/S0141-0296(00)00068-7

[14] Taucer, F.F., Spacone, E., Filippou, F.C.: A Fiber beam-column element for seismic response analysis of reinforced concrete structures", Report No. UCB/EERC-91/17, Earthquake Engineering Research Center, College of Engineering, University of California Berkeley, 1991.

[15] Petrangeli, M.: Fiber element for cyclic bending and shear of RC structures, II: Verification, Journal of Engineering Mechanics (ASCE), 125 (9), pp. 1002-1009, 1999., http://dx.doi.org/10.1061/(ASCE)0733-9399(1999)125:9(1002)

[16] Jeong, S.H., Elnashai, A.S.: Analytical assessment of an irregular RC frame for full-scale 3d pseudo-dynamic testing part i: analytical model verification, Journal of Earthquake Engineering, 9 (1), pp. 95-128, 2005., http://dx.doi.org/10.1080/13632460509350535

[17] Mwafy, A.: Assessment of seismic design response factors of concrete wall buildings, Earthquake Engineering and Engineering Vibration, 10, pp. 115-127, 2011., http://dx.doi.org/10.1007/s11803-011-0051-7

[18] Duan, H., Hueste, M.B.D.: Seismic performance of a reinforced concrete frame building in China, Engineering Structures, 41, pp. 77-89, 2012.

[19] Kwon, O.S., Kim, E.: Case study: Analytical investigation on the failure of a two-story RC building damaged during the 2007 Pisco-Chincha earthquake, Engineering Structures, 32, pp. 1876-1887, 2010., http://dx.doi.org/10.1016/j.engstruct.2009.12.022

[20] Sarno, L.D., Manfredi, G.: Seismic retrofitting with buckling restrained braces: Application to an existing non-ductile RC framed building, Soil Dynamics and Earthquake Engineering, 30, pp. 1279–1297, 2010., http://dx.doi.org/10.1016/j.soildyn.2010.06.001

[21] Yön, B., Calayır, Y.: Pushover Analysis of a Reinforced Concrete Building According to Various Hinge Models, 2nd International Balkans Conference on Challenges of Civil Engineering, BCCCE, Tirana, pp. 1-10, 2013.

[22] Carvalho, G., Bento, R., Bhatt, C.: Nonlinear static and dynamic analyses of reinforced concrete buildings - comparison of different modelling approaches, Earthquakes and Structures, 4 (5), pp. 451-470, 2013., http://dx.doi.org/10.12989/eas.2013.4.5.451

[23] Yön, B., Calayır, Y.: Effects of confinement reinforcement and concrete strength on nonlinear behaviour of RC buildings, Computers and Concrete, 14(3), pp. 279-297, 2014., http://dx.doi.org/10.12989/cac.2014.14.3.279

[24] SeismoStruct v7: A computer program developed for the accurate analytical assessment of structures, subjected to earthquake strong motion. Available at: www.seismosoft.com [September 8, 2014]

[25] SeismoArtif v2.1: A computer program for generating artificial earthquake accelerograms matched to a specific target response spectrum. Available at: www.seismosoft.com [July 19, 2013]

[26] TS 498: Design Loads for Buildings, Turkish Standards Institute, Ankara, Turkey

[27] Mander, J.B., Priestley, M.J.N., Park, R.: Theoretical stress-strain model for confined concrete, Journal of Structural Engineering (ASCE), pp. 1804–1826, 1988., http://dx.doi.org/10.1061/(ASCE)0733-9445(1988)114:8(1804)

[28] PEER Strong Ground Motion Database, peer.berkeley.edu/smcat/search.html

[29] Eurocode 8: Design of structures for earthquake resistance Part 1: General rules, seismic actions and rules for buildings

[30] SeismoSignal v5.1 - A computer program for the processing of strong-motion data. Available at: www.seismosoft.com [July 19, 2013]